

# THE RELATIONSHIP BETWEEN ENERGY CONSUMPTION AND SURFACE TEMPERATURE: COMBINING MULTIPLE-SCALE OBSERVATIONS

Takahiro Yoshida <sup>1\*</sup>, Soowon Chang <sup>1,2</sup>, Daisuke Murakami <sup>3</sup>, Yoshiki Yamagata <sup>1</sup>

<sup>1</sup> Center for Global Environmental Research, National Institute for Environmental Studies, Tsukuba, Japan

<sup>2</sup> School of Building Construction, Georgia Institute of Technology, Atlanta, GA, USA

<sup>3</sup> Department of Data Science, The Institute of Statistical Mathematics, Tokyo, Japan

\* (Corresponding Author)

## ABSTRACT

The relationship between air temperature and energy consumption at the city level has been investigated to better understand the impact of the climate change on energy demands. Temperature rising caused by the climate change has been shown to lead to the increase of building energy demands. Buildings also contribute to climate change by radiating heat from building surfaces. In this respect, this study aims to evaluate the potential impact of building rooftop and façade surface temperatures on household energy consumption. We developed a method that combines multiple scale observations, including an Internet of things (IoT) sensor network and remote sensing, to estimate the relationship between surface temperatures and energy consumption. The results will contribute to managing building energy uses based on the better understanding of micro-scale temperature effects in urban area.

**Keywords:** energy consumption, surface temperature, building façade, remote sensing, airborne monitoring

## 1. INTRODUCTION

Effective action plans should be developed to manage energy consumption and demands in residential sectors [1]. It is important to understand both energy consumption usage patterns and temperatures, as residents sometimes control household temperatures with air conditioners, further increasing energy costs [2]. Given the need for sustainable urban environmental systems design, and the negative effects of high local

temperatures on human health and wellbeing, it is also considered necessary to evaluate urban microclimates [3].

As reviewed by Belussi et al. [4], many studies have looked at the relationship between air temperature and energy consumption at the city level, and how increasing energy demands may impact climate change [5–7]. For example, Fung et al. [8] found that rising air temperature had a significant impact on the energy sector in Hong Kong. Among many reasons increasing air temperatures, building surface temperatures influence air temperature changes and building energy demands [9]. Surface temperature influences on the urban heat-island impacts directly by radiating heat, and this micro-climate changes affect building energy demands [10]. Moreover, building surface temperatures influence the indoor building energy use through heat conduction. When surface temperature high, buildings require low energy during heating period, but they require high energy during the cooling seasons [11].

Building surface temperature also influence mean radiant temperature and this contributes to pedestrian thermal comfort [12]. Evaluating both air temperatures and building surface temperatures will contribute to better understanding of the more detailed micro-scale relationships as well as including a human-experiential perspective. Due to the growing distribution of the Internet of things (IoT) sensor networks, micro-scale data has enabled us to observe multi-scale temperatures [13,14]. Furthermore, we can also easily obtain surface temperature data from multiple scale remote sensing systems [15].

In this study, as a first step in the evaluation of micro-scale temperature-energy relationships, we installed IoT network sensors on households and combined the collected data with that obtained from multiple surface monitoring systems. The study took place in the Kyojima district, Sumida ward, Tokyo, Japan. The target data is from August 28, 2017, which was a sunny day with minimum and maximum air temperatures of 22.3 and 31.4 degrees, respectively.

## 2. SURFACE TEMPERATURE MONITORING

### 2.1 Review of heatwave-related monitoring in Japan

In Japan, climate conditions are monitored in multiple ways. For example, Japan's Meteorological Agency monitors temperature, humidity, and other atmospheric variables in about 1,300 stations using AMeDAS (Automated Meteorological Data Acquisition System).

Weather has often been monitored using a bottom-up approach. For example, Weather News Inc. collects weather information from 2.5 million voluntary weather reporters. Indoor and outdoor weather information collected by IoT devices in and/or around houses is uploaded using a portal site (i.e. NETATMO Inc.). Use of Volunteered Geographic Information (VGI) is now spreading widely all over the world [16]. Remote sensors such as MODIS (resolution: 500 m), ASTER (resolution: 90 m), and LANDSAT 8 (resolution: 30 m) have also been used to monitor surface temperatures with a relatively high-spatial resolution.

Despite increases in heat-related monitoring systems, they are not yet sufficient for monitoring heatwave events in district levels, as the capability to measure these events depends on the location of micro-scale urban structures such as buildings and trees. Therefore, this study attempted to estimate micro-scale heat conditions by combining airborne and tower monitoring techniques, as explained below.

### 2.2 Tower monitoring

We used tower monitoring data in collaboration with the Japan Weather Association to monitor temporal surface temperature changes. An InfReC R500EX thermos camera provided by Nippon Avionics Co. Ltd. was installed at an altitude of 480m on the Tokyo SkyTree. Ground temperatures were monitored over 5 minute intervals on the East side of the SkyTree.

As shown in Fig. 1 (a), each plot recorded the temperature at 11:00, 13:00, and 15:00. This figure confirmed that the monitored images captured rapid temperature increase at around the noon. While data

was recorded in 5 minute intervals, we used images from 2 hour intervals (1:00, 3:00, ..., 23:00).

### 2.3 Airborne monitoring

To monitor micro-scale heatwaves, we used an airborne monitoring technique in collaboration with SkyMap Co. Ltd. The target monitoring time-period was between 11:01 and 11:43 on August 28, 2017. The flight path was a zig-zag pattern over the East side of the Tokyo SkyTree in the Sumida ward, in the north-east part of Tokyo, Japan.

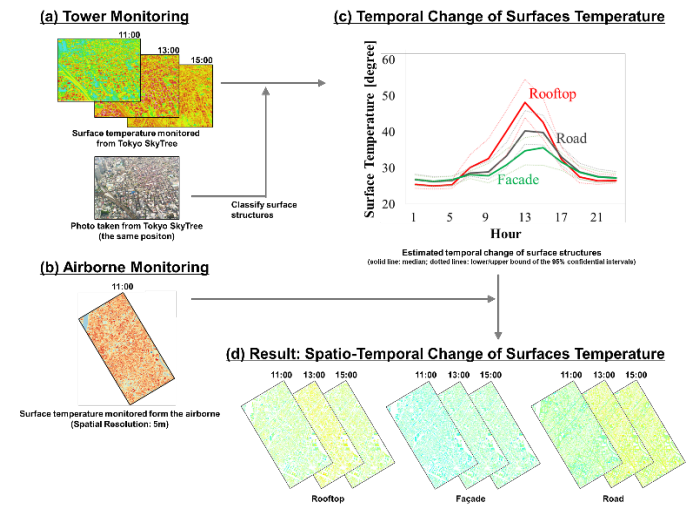


Fig. 1 Processing method used to monitor spatio-temporal surface temperature changes using tower and airborne monitoring techniques.

Monitored images were then combined using mosaic processing.

In Fig. 1 (b), the resulting surface temperature map demonstrates that the monitoring technique successfully captured high temperatures on rooftops, low temperatures in rivers, and so on. Unfortunately, airborne monitoring is costly, so it is unrealistic to monitor temperatures over an entire day. The next section introduces another monitoring technique that is able to better measure the temporal behavior of surface temperatures.

### 2.4 Processing of heat monitoring data

Tower monitoring and airborne monitoring have different limitations. Using the former, monitoring images are inclined, whereas the latter is only available over a limited time-period, and is not necessarily straightforward for heatwave management applications. In addition, the former covers only a small portion of the airborne monitoring area.

Thus, we combined these two monitoring techniques to compensate for their respective shortcomings, and to quantify high-resolution, spatio-temporal heat intensity. In regard to the tower monitoring images, (i) the image cells were clustered based on monitored temporal patterns. Based on the results road, rooftop, and façade temporal temperature variations were modeled. In the case of airborne monitoring images, (ii) spatial patterns of road and rooftop temperatures were modeled at 11:20, which was the time of the mean daytime temperatures. After that, (iii) surface temperature maps were created for 2 hour periods by combining the results from (i) and (ii) through histogram matching.

#### 2.4.1 Processing of the tower monitoring images

The tower monitoring cell images were clustered based on temporal temperature variation. We applied  $k$ -means clustering, which is a standard clustering algorithm. Based on a preliminary analysis, the number of clusters was fixed at four. We first tried to optimize the number of clusters by minimizing the Akaike Information Criterion, which is a well-known generalization error statistic, but the resulting number of clusters was too high, and the clusters were difficult to interpret. The final estimated clusters were fit to a photo, as shown in Fig. 1 (a).

Monitored rooftop, road, and façade cluster temperatures were aggregated at each time point, and the median values and the 95 % confidential intervals were plotted in Fig. 1 (c). While the surface temperatures in each cluster were similar overnight, they had substantial differences in the daytime; rooftops were the hottest, roads were moderate, and façades were the coolest among the three. It was also shown that the surface temperature were more uncertain (i.e., wide 95 percent intervals) during the day, compared to at night. These results are intuitively reasonable. One of our interesting findings was that the hottest time shifts depended on surface type: rooftop temperatures had a sharp peak at around 13:00, road temperatures had a relatively flat peak between 13:00 and 15:00, and façade temperatures had a peak at around 15:00. This result might be because rooftops receive the most solar radiation, and the heat saturates more quickly there than on roads and façades. The late façade peak might be because they usually receive stronger direct sunlight after the sun starts setting.

The aforementioned results highlight the effectiveness of tower monitoring for capturing

temporal patterns by surface structure type. It is important to note that the façade temperatures were never monitored using the common (orthogonal) remote sensing technique. Observed façade temperatures were more likely to explain the influence of outdoor heat on the indoor environment (through walls/window) than on road and rooftop temperatures. Tower monitoring is, therefore, an important tool for monitoring indoor heat stress.

To combine the tower and airborne monitoring results, 1%, 2%, ..., 100% temperature cluster quantiles were calculated.

#### 2.4.2 Processing of the airborne image

The building polygons, which were provided by Zenrin Co. Ltd., were overlain on the airborne images, and 1%, 2%, ..., 100% temperature quantiles for the rooftops were determined. Likewise, 1%, 2%, ..., 100% road temperature quantiles are also calculated. As we did not have road surface data, we assumed that areas other than buildings, green areas, and rivers (source: National Land Numerical Information downloads service) were roads.

### *2.5 Surface temperature mapping*

The temperature quantiles for rooftops and roads from the tower and airborne images were then combined by matching the quantiles. The procedure for calculating rooftop temperatures was as follows: (i) for the tower monitoring images, the quantile values at 11:20 were estimated using temporally linear interpolation based on the tower monitoring images at 11:00 and 13:00; (ii) for each quantile  $\tau$ , the change in temperature relative to 11:20, defined by  $c(t, \tau) = [\text{the } \tau\text{-th quantile temperature value at time } t] / [\text{the } \tau\text{-th quantile temperature value at time } 11:20]$ , was evaluated over 2 hours using the tower monitoring images; (iii) for an airborne monitoring rooftop cell image, whose temperature is at the  $\tau$ -th quantile, the temperature at  $t$ -th time was estimated by multiplying the temperature monitored at 11:20 with  $c(t, \tau)$ ; (iv) the same estimation was done for all the cells. The same calculation was done to estimate road temperature as well. Finally, the estimated rooftop and road temperatures were merged using mosaic processing. In short, surface temperatures were estimated so that temporal patterns in each quantile, which were monitored through tower monitoring, and spatial patterns in each quantile, which were monitored by airborne monitoring, were preserved.

The estimated surface temperatures increased rapidly between 11:00 and 13:00, and remained high until around 17:00, when they began to gradually decrease. We also found that road temperatures remained relatively high through the night, whereas rooftop temperatures were higher throughout the day.

As previously mentioned, façade temperatures monitored using tower monitoring are potentially useful for estimating indoor heat stress. Therefore, we then estimated façade temperatures on each building. To achieve this, we estimated: [façade temperature at  $t$ -th time at  $g$ -th cell] = [rooftop temperature at  $t$ -th time at  $g$ -th cell]  $\times$  [(façade temperature at  $t$ -th time at  $\tau(g)$ -th quantile)/(rooftop temperature at  $t$ -th time at  $\tau(g)$ -th quantile), where  $\tau(g)$  represents the quantile of the monitored value at the  $g$ -th cell. The quantile was calculated using airborne cells on buildings.

### 3. ENERGY CONSUMPTION MONITORING

We used two types of sensors to collect data using IoT technology; one is a networked sensor that sends collected data in nearly real-time, and the other is non-networked sensor with an SD storage card inside, where someone manually collects the data from the storage card. IoT data collection from the different types of devices can avoid security issues in the future [17]. We set all the sensors to record over the same time-period (August 28, 2017) that was used for heat monitoring (mentioned in Section 2).

We installed the sensors on seven households in Kyojima: five in newly built apartment buildings and two in wooden houses.

To measure electricity consumption, networked sensors were installed to each household's switchboard with clamps. We also used smart meters made by Sessor Inc., which recorded data in 1-minute intervals. The data was then sent to a central database via a Wi-Fi network.

### 4. RESULT AND DISCUSSION

Fig. 2 shows temporal variation between energy consumption (collected using IoT sensor network) and rooftop and façade surface temperatures (collected using tower and airborne monitoring), on August 28, 2017. The wooden house had both higher surface temperatures and lower energy consumption rates than the apartment. Therefore, although we first applied a vector autoregression (VAR) model to estimate energy consumption, based on the regressions of the two surface temperatures, the change-ratio, and the 1<sup>st</sup> and 2<sup>nd</sup> lags, the results from the apartment and wooden house were not statistically significant. However, only

the 2<sup>nd</sup> lag in the rooftop temperatures recorded from the wooden house was significant at a 5% level. These results suggest that in order to better support urban energy demand management for the residential sector, surface temperatures monitored two hours prior should help predict energy consumption. Refinement of this estimation method should be researched further in the future.

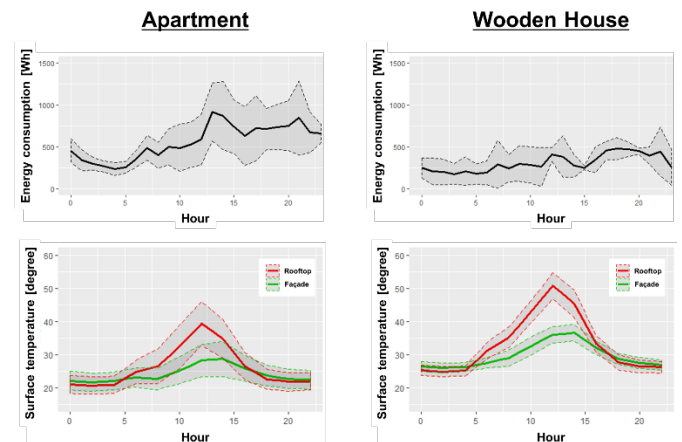


Fig. 2 Temporal variation of energy consumption [Wh] collected by an IoT sensor network and rooftop and façade surface temperatures [degree] collected via tower and airborne monitoring, on August 28, 2017. (solid line: mean; dotted lines: lower and upper bound of standard deviation)

### REFERENCE

- [1] Matsui K, Yamagata Y, Kawakubo S. Real-time sensing in residential area using IoT technology for finding usage patterns to suggest action plan to conserve energy. *Energy Procedia* 2019;158:6438–45. doi:10.1016/J.EGYPRO.2019.01.171.
- [2] Gottwalt S, Ketter W, Block C, Collins J, Weinhardt C. Demand side management—A simulation of household behavior under variable prices. *Energy Policy* 2011;39:8163–74. doi:10.1016/J.ENPOL.2011.10.016.
- [3] Zeng F, Gao N. Use of an Energy Balance Model for Studying Urban Surface Temperature at Microscale. *Procedia Eng* 2017;205:2956–66. doi:10.1016/J.PROENG.2017.10.113.
- [4] Belussi L, Barozzi B, Bellazzi A, Danza L, Devitofrancesco A, Fanciulli C, et al. A review of performance of zero energy buildings and energy efficiency solutions. *J Build Eng* 2019;25:100772. doi:10.1016/J.JOBE.2019.100772.
- [5] Wong N., Cheong DK., Yan H, Soh J, Ong C., Sia A. The effects of rooftop garden on energy consumption of a commercial building in Singapore. *Energy Build*

2003;35:353–64. doi:10.1016/S0378-7788(02)00108-1.

[6] Santamouris M, Papanikolaou N, Livada I, Koronakis I, Georgakis C, Argiriou A, et al. On the impact of urban climate on the energy consumption of buildings. *Sol Energy* 2001;70:201–16. doi:10.1016/S0038-092X(00)00095-5.

[7] Li J, Yang L, Long H. Climatic impacts on energy consumption: Intensive and extensive margins. *Energy Econ* 2018;71:332–43. doi:10.1016/J.ENERCO.2018.03.010.

[8] Fung WY, Lam KS, Hung WT, Pang SW, Lee YL. Impact of urban temperature on energy consumption of Hong Kong. *Energy* 2006;31:2623–37. doi:10.1016/J.ENERGY.2005.12.009.

[9] Castleton HF, Stovin V, Beck SBM, Davison JB. Green roofs; building energy savings and the potential for retrofit. *Energy Build* 2010;42:1582–91. doi:10.1016/J.ENBUILD.2010.05.004.

[10] Prado RTA, Ferreira FL. Measurement of albedo and analysis of its influence the surface temperature of building roof materials. *Energy Build* 2005;37:295–300. doi:10.1016/J.ENBUILD.2004.03.009.

[11] Ascione F, Bianco N, de' Rossi F, Turni G, Vanoli GP. Green roofs in European climates. Are effective solutions for the energy savings in air-conditioning? *Appl Energy* 2013;104:845–59. doi:10.1016/J.APENERGY.2012.11.068.

[12] Park CY, Lee DK, Krayenhoff ES, Heo HK, Ahn S, Asawa T, et al. A multilayer mean radiant temperature model for pedestrians in a street canyon with trees. *Build Environ* 2018;141:298–309. doi:10.1016/J.BUILDENV.2018.05.058.

[13] Murakami D, Yamagata Y, Yoshida T, Matsui T. Optimization of local microgrid model for energy sharing considering daily variations in supply and demand. *Energy Procedia* 2019;158:4109–14. doi:10.1016/J.EGYPRO.2019.01.823.

[14] Yoshida T, Yamagata Y, Murakami D. Energy demand estimation using quasi-real-time people activity data. *Energy Procedia* 2019;158:4172–7. doi:10.1016/J.EGYPRO.2019.01.813.

[15] Murakami D, Yamagata Y, Yoshida T. Spatio-temporal heatwave risk modeling combining multiple observations. *Proc. 2019 IEEE Geosci. Remote Sens. Soc. Symp. 2019, 2019*, p. In Press.

[16] Flanagan AJ, Metzger MJ. The credibility of volunteered geographic information. *GeoJournal* 2008;72:137–48. doi:10.1007/s10708-008-9188-y.

[17] Rathore MM, Ahmad A, Paul A, Rho S. Urban planning and building smart cities based on the Internet

of Things using Big Data analytics. *Comput Networks* 2016;101:63–80. doi:10.1016/J.COMNET.2015.12.023.